

Dense cores in the ρ Ophiuchi main cloud

A. Abergel¹, P. André⁴, J.P. Bernard¹, F. Boulanger¹, F.X. Désert¹, E. Falgarone²,
G. Lagache¹, L. Nordh³, G. Olofsson³, M. Perault², J.-L. Puget¹, W.T. Reach¹, I. Ristorcelli⁵

- (1) Institut d'Astrophysique Spatiale, Université Paris-Sud, Bât.121, 91405, Orsay, France
(E-mail: abergel@ias.fr, Tel: 33 01 69 85 85 66, Fax: 01 69 85 86 79)
(2) Radioastr. Millimétrique, Ecole Normale Supérieure, 24 rue Lhomond, 75005 Paris, France
(3) Stockholm Observatory, S-133 36 Saltsjöbaden, Sweden
(4) Service d'Astrophysique, Centre d'Etudes de Saclay, 91191 Gif-Sur-Yvette Cedex, France
(5) CESR, UPR-CNRS 8002, 9 avenue du colonel Roche, 31029 Toulouse Cedex, France

Abstract

ISOCAM observations of the ρ Ophiuchi main cloud L1688 conducted in the two broad-band filters LW2 (5-8.5 μm) and LW3 (12-18 μm) have revealed numerous dense cores seen as sharp and deep absorption structures against the diffuse cloud background. Such cores are believed to be stellar progenitors. A preliminary analysis for one selected core shows that the density structure, modeled in a spherical geometry and derived from the opacity profile, is steeper than r^{-2} . This could indicate the influence of external pressure on the core structure. The SPM/PRONAOS balloon-borne observations have measured the emission spectra of such cores, and demonstrated that they are significantly colder than the ambient medium. FIRST will allow an unprecedented mapping of these objects which are strong sources of sub-mm emission at small scale (typically 1 arcmin).

1 Introduction

The understanding of the physical properties of dense cores in molecular clouds is a critical issue in the theory of star formation, since these objects are believed to be stellar progenitors. In the ρ Ophiuchi main cloud L1688, several dense cores have been found in HCO⁺ and DC⁺ emission lines (Loren & Wootten 1986, Loren et al. 1990, hereafter LWW) and in the submillimeter continuum emission mainly at 1.3 mm (Mezger et al. 1992, Motte et al. 1997). However, these observations have a limited signal to noise ratio and/or angular resolution. The most recent 1.3 mm observations made at IRAM (Motte et al. 1997) have an angular resolution (11'') which allow to study the densest internal parts of the cores, but are limited by sensitivity in the outer parts so that the density structure close to the interface with

the ambient molecular cloud is poorly constrained. Moreover the whole emission spectrum of these cores have never been measured.

The IR camera ISOCAM of the ISO satellite (Cesarsky et al. 1986) and the SPM/PRONAOS balloon-borne experiment (Serra et al., this conference) give an unprecedented view on dense cores. L1688 is mainly illuminated from the far side of the cloud, so the ISOCAM observations conducted in the two broad-band filters LW2 (5-8.5 μm , centered to 6.75 μm) and LW3 (12-18 μm , centered to 15 μm) have revealed numerous dense cores seen in absorption (Fig. 1 from Abergel et al. 1996). The extinction structures are observed with the very high angular resolution (6 arcsec for ρ Oph) and sensitivity of ISOCAM (section 3), and without any biases intrinsic to each density tracer since the extinction is due to the whole column density on the line of sight.

We show in section 4 that the opacity profiles measured across these cores by ISOCAM allow to derive their density structure, especially in the interface regions between the cores and the surrounding medium. The density profiles which are deduced give new constraints for the early stage of the star formation, since a r^{-2} profile is compatible with an isothermal self-gravitating sphere while a steeper profile reveal external pressure.

We discuss in section 5 the observations of the SPM/PRONAOS balloon-borne experiment. For the first time the submillimeter spectrum of the densest cores of L1688 have been measured. The low values of the temperature which are deduced represent a strong constrain on the physical properties of the cores, and demonstrate that these objects are strong sources of sub-mm emission at small scale (1 arcmin).

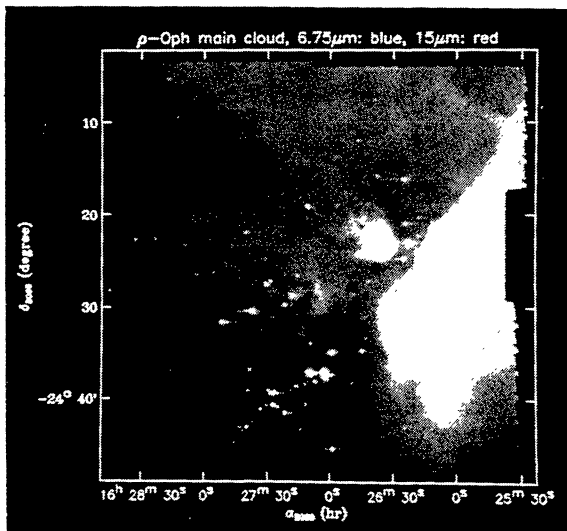


Figure 1: ISOCAM map at $6.75 \mu\text{m}$ and $15 \mu\text{m}$ (coded in blue and red respectively), from Abergel et al. 1996.

2 The ρ Oph main cloud

The ρ Oph region is one of the nearest (160 pc, Bertiau 1958) extended molecular complex located at high Galactic latitude ($b \simeq 17^\circ$). The main cloud (L1688) is totally opaque on optical plates and harbors some of the brightest spots of the Solar Neighborhood in the ^{12}CO , ^{13}CO and C^{18}O lines (Encrenaz et al. 1975, Wilking & Lada 1983, Loren 1989). The molecular complex is heated on large scales by the nearby Sco OB2 association (de Geus et al. 1989). The main cloud is known to contain a few young embedded B stars (two have been previously detected in the field mapped by ISOCAM) and extremely numerous Young Stellar Objects (YSOs) previously identified in the near IR (Wilking et al. 1989, Greene & Young 1992, see also Fig. 1). The unusually high IR brightness of L1688 is due to large column densities (A_v up to 100) combined with the presence of early type stars and YSOs.

3 Absorption features revealed by ISOCAM

The Sco OB2 association is located mainly behind the cloud (de Geus et al. 1989) and could be responsible for a global illumination of the far side of the cloud. This particular geometry therefore provides a unique opportunity of detecting opaque cores in ab-

sorption against the large scale diffuse background emission. Since the extinction around $7 \mu\text{m}$ is typically 50 times lower than at visible wavelengths, the detection of absorption features implies the existence of very high column densities. The deepest absorption features visible on the ISOCAM map (close to $\alpha_{2000} = 16^{\text{h}}27^{\text{m}}30^{\text{s}}$, $\delta_{2000} = -24^\circ 27'$, see Fig. 1) coincides with the DCO^+ and sub-mm B1 and B2 dense cores (LWW). Small scale deep absorptions are also visible around $\alpha_{2000} = 16^{\text{h}}28^{\text{m}}30^{\text{s}}$, $\delta_{2000} = -24^\circ 19'$ and correspond to the DCO^+ core Oph D (Fig. 2).

A large number of small scale absorptions features are also detectable in the ISOCAM field with a lower contrast, especially in the southern part of the C^{18}O ridge (Wilking & Lada, 1983) around the dense cores Oph C, Oph E and Oph F observed in DCO^+ by LWW and recently mapped by Motte et al. (1997) at 1.3 mm. The broad elongated ^{13}CO filament extending from the bright emission (at $\alpha_{2000} \sim 16^{\text{h}}26^{\text{m}}34^{\text{s}}$, $\delta_{2000} \sim -24^\circ 23'30''$) toward the North-East (Loren 1989) is also visible as a large scale absorption feature in the ISOCAM map.

4 Density structure

To derive the opacity profiles $\tau(r)$ of the cores from their brightness profiles, we need to estimate as well as possible the background and foreground emissions. Therefore we have chosen to work on the dense core Oph D ($\alpha_{2000} = 16^{\text{h}}28^{\text{m}}30^{\text{s}}$, $\delta_{2000} = -24^\circ 19'$) which does not appear to be included in a region containing strong IR color variations or embedded objects (Figs. 1-2).

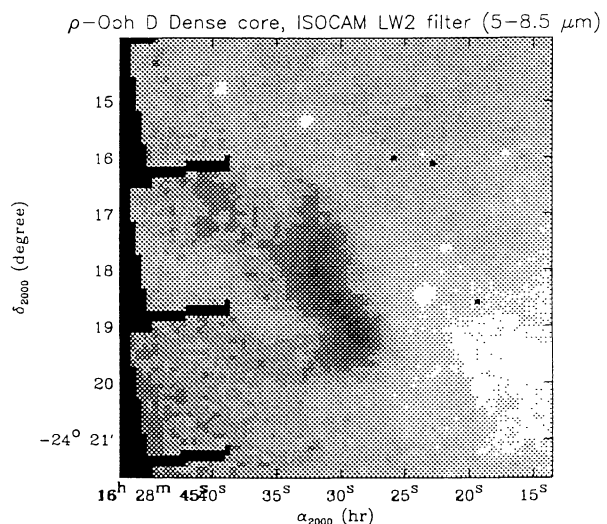


Figure 2: Oph D dense cloud in the LW2 filter (centered to $6.75 \mu\text{m}$)

The foreground emission contains the zodiacal emission and the emission coming from the near side of the dense cloud. To estimate the zodiacal emission, we use the model of Reach et al. (1995) calibrated from the DIRBE/COBE data. This model gives at the time of ISOCAM observations a zodiacal emission equal to 5.7 ± 1 and 45 ± 9 MJysr $^{-1}$ at $6.75 \mu\text{m}$ and $15 \mu\text{m}$ respectively ($\beta \simeq -2.5^\circ$). However, the minimal brightnesses observed in our maps (near the bottom left corner of Fig. 1: $I_\nu(6.75\mu\text{m}) = 8.6$ and $I_\nu(15\mu\text{m}) = 39$ MJysr $^{-1}$) give a stronger constrain for the zodiacal emission at $15 \mu\text{m}$: 39^{+0}_{-3} MJysr $^{-1}$. The contribution of the dust located at the near side of the cloud is unknown, but we can use as an upper limit the minimal brightness of the core. Finally we obtain a total foreground emission for Oph D in the range 5.7-8.9 MJysr $^{-1}$ and 39-40.7 MJysr $^{-1}$ at $6.75 \mu\text{m}$ and $15 \mu\text{m}$ respectively.

The density structure of Oph D is modeled in a spherical geometry to fit the observed profile: a constant local density n_0 up to a radius r_0 , and a power law decrease $n(r) = n_0(r_0/r)^\beta$ down to the density of the surrounding gas n_{out} estimated to be 10^4 cm^{-3} according to the ^{13}CO observations of Loren (1989). The computed column densities are converted in opacities using the standard values of $\lambda\tau/N_H$ for graphite and silicate spheres (Draine & Lee 1984). The free parameters n_0 and r_0 are adjusted in order to fit the computed $\tau(r)$ profile with the opacity profile determined from the data.

An example is presented on figure 3. The width of the opacity profiles is typically 0.1 pc (2.1 arcmin). In the following, we concentrate our analysis on the right sides of the profiles, since they are generally steeper than the left ones. The best fits are obtained with $\beta = 3$ for the two filters. The agreement is better with $\beta = 3$ than $\beta = 2$ for all the horizontal profiles with significant extinction, and whatever the assumed value of the foreground emission is (in the range discussed before). The value of β is strongly constrained by the wings of the profiles corresponding to the interface regions between the dense core and the surrounding dust, not by the central opacities, indicating that such an analysis is only possible with high signal to noise data. The only way to obtain a good agreement of the opacity profiles using $\beta = 2$ is to assumed that n_{out} is around $5 \cdot 10^4 \text{ cm}^{-3}$, which is in conflict with the determination of Loren (1989).

For the example of Fig. 3, we consider that there is no contribution coming from the near side of the cloud (only the zodiacal emission is removed). The adjusted values of the parameters are (for $\beta = 3$): $n_0 = 1.2 \cdot 10^6 \text{ cm}^{-3}$, $r_0 = 0.013 \text{ pc}$, $N_H = 1.5 \cdot 10^{23} \text{ cm}^{-2}$, and $n_0 = 8.3 \cdot 10^5 \text{ cm}^{-3}$, $r_0 = 0.016 \text{ pc}$, $N_H = 1.2 \cdot 10^{23} \text{ cm}^{-2}$ from the extinction profiles at $6.75 \mu\text{m}$ and $15 \mu\text{m}$ respectively. The central density n_0 and the

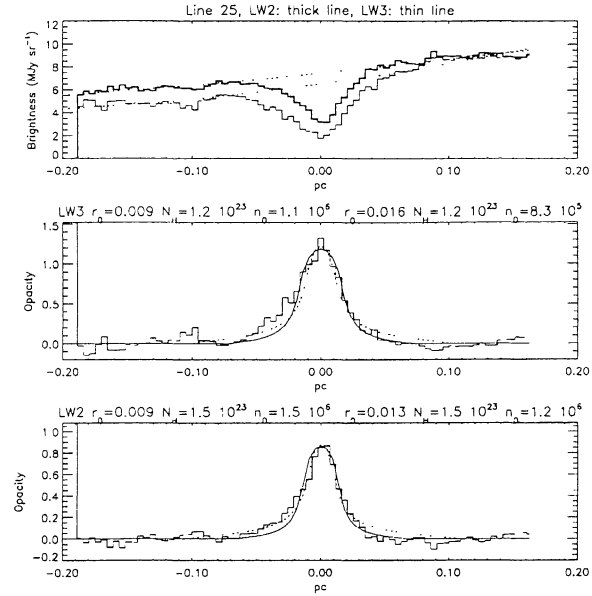


Figure 3: Upper panel: Horizontal profiles across Oph D at $6.75 \mu\text{m}$ (thick line) and $15 \mu\text{m}$ (thin line), after removing the zodiacal emission. A baseline (dotted line) is subtracted before computing the opacity profile.

Lower panel: Opacity profiles for the LW2 and LW3 filters. In this case the foreground emission is assumed to be equal to the zodiacal emission. The dotted and solid lines show the result of our modeling with $\beta = 2$ and 3 respectively (the adjusted parameters are given on top of the panel). Only the right sides of the profiles are adjusted. The best agreements are obtained with $\beta = 3$ (solid lines).

central column density N_H are comparable to values deduced from sub-mm or molecular observations of dense cores (LWW, Mezger et al. 1992, Motte et al. 1997). We see that the values are similar for the two filters, which shows that the wavelength dependence of $\lambda\tau/N_H$ given by Draine & Lee 1984 in the range $5\text{-}18 \mu\text{m}$ quantitatively explain the difference of extinction observed for the two filters.

5 Sub-mm emission

During its first successful flight, the balloon-borne experiment PRONAOS with the SPM four channels sub-mm photometer has detected with a spatial resolution in the range 2-3.5 arcmin several cold condensations in the ρ Oph main cloud (Ristorcelli et al. 1996, Serra et al. 1997). These condensations precisely peak at the location of the deepest ab-

sorption features revealed by ISOCAM (especially around Oph B and Oph C, see Fig. 4), showing that the sub-mm emission excesses detected by SPM are due to the dense cores seen in absorption with ISOCAM. Values of the temperatures as low as 12 K are deduced from the measured spectra (typically 12 K with a spectral index of 2, see Ristorcelli et al. 1996), which could indicate a strong decrease of the temperature in the cores, down to even lower temperature because the cores (typically 1 arcmin) are diluted in the beam (2-3.5 arcmin). Combined with the steep increase of the local density revealed by ISOCAM, these observations should constrain the radiative transfer and the spatial variations of the grain properties inside the cores.

Lagache et al. (1997) have shown that the densest parts of most of molecular complexes contain dust at a temperature lower than in the external regions. PHOC and BOL will give an unbiased survey of such cold condensations in a spectral range covering their whole emission spectrum (André, this conference). The spatial variations of the emission properties of the dust will be monitored from the external to the internal parts of the cores.

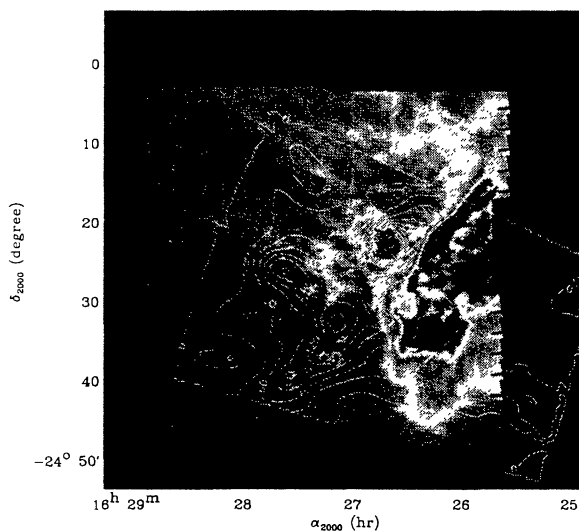


Figure 4: ISOCAM map compared to the 540-1100 emission measured with SPM-PRONAOS (Serra et al., this conference). The SPM contours are drawn with a step of 30MJy/sr.

References

Abergel A., et al., 1996, A&A 315, L329
 André P., Deeney B.D., Philips R.B. et al., 1992, ApJ 401, 667

André P., Ward-Thompson D., Barsony M., 1993, ApJ 406, 122
 Bertiau F.C., 1958, ApJ 128, 533
 Brown R.L., Zuckerman B., 1995, ApJ 202, L125
 Cesarsky, C.J. et al., 1996, A&A 315, L32
 de Geus E.J., Zeeuw P.T., Lub J., 1989, A&A 216, 44
 Draine B.T., Lee H.M., 1984, ApJ 285, 89
 Encrenaz P.J., Falgarone E., Lucas R., 1975, A&A 44, 73
 Falgarone E., & Gilmore W. 1981 A&A 95 32
 Greene T.P., Young E.T., 1992, ApJ 395, 516
 Lagache G., Abergel A., Boulanger F., Puget J.-L. 1997, this conference
 Loren R.B., 1989, ApJ 338, 902
 Loren R.B., Wootten A., 1986, ApJ 306, 142
 Loren R.B., Wootten A., Wilking B.A., 1990, ApJ 365, 269
 Mezger P.G., Sievers A., Zylka R. et al., 1992, A&A 265, 743
 Motte F., André P., Neri R., 1997, in preparation
 Reach W.T et al. 1995. In Dwek E. (ed.) Unveiling the cosmic infrared background. AIP press, New York, p. 37
 Ristorcelli et al. 1996. IRTS Symposium, Tokyo, Japan
 Serra et al. 1997, this conference
 Wilking B.A., Lada C.J., Young E.T. 1989, ApJ 340, 823